

# Modeling of the interaction between the electromagnetic field of a combined resonator and biowastes during ultrahigh frequency heating

Natalia Kosulina<sup>1\*</sup> , Mykola Lysychenko<sup>1</sup> , Maksym Sorokin<sup>1</sup> ,  
Yuri Handola<sup>1</sup> , Stanislav Kosulin<sup>1</sup> , Mariia Chorna<sup>1</sup> 

<sup>1</sup> Department of Electromechanics, Robotics, Biomedical and Electrical Engineering State Biotechnological University, Kharkiv, Ukraine

\* Corresponding author's e-mail: kosnatgen@ukr.net

## ABSTRACT

The object of the research is the process of ultrahigh-frequency (UHF) treatment of livestock production biowaste aimed at its disinfection and energy-efficient processing. The problem lies in the absence of scientifically grounded methods for designing continuous-flow UHF installations capable of providing uniform heating of biowaste of varying composition with minimal energy consumption and without loss of nutritional value. As a result of the conducted theoretical and experimental studies, the dielectric properties of different types of biowaste (fat, blood, bones) were analyzed, and their influence on the efficiency of electromagnetic energy absorption was determined. The aim of the work was to establish the regularities of interaction between the electromagnetic field of a combined resonator and biowaste to enhance the energy efficiency of the process. The dielectric parameters of biowaste ( $\epsilon' = 50\text{--}60$ ;  $\epsilon'' = 10\text{--}25$ ) and the electrodynamic characteristics of resonators of various geometries were determined. It was found that a combined «hemisphere + cylinder» resonator provides a quality factor  $Q = 6910\text{--}9270$  and an electric field strength  $E = 0.6\text{--}3.5$  kV/cm, which increases energy efficiency by 15–18% compared to the cylindrical type. A mathematical model of the electric field distribution and a heating model were developed. Strong correlations  $\epsilon' - Q$  ( $r = 0.93$ ) and  $\epsilon'' - E$  ( $r = 0.88$ ) were obtained, explaining the interdependence between electrophysical and resonator parameters. The obtained results are distinguished by a comprehensive approach to process modeling and the possibility of dynamic regulation of UHF field parameters, which prevents overheating or underheating of the material. The practical significance of the results lies in the development of energy-saving, environmentally safe next-generation UHF installations for the disinfection and processing of biowaste under farm, pilot, and industrial conditions.

**Keywords:** ultrahigh-frequency treatment, combined resonator, biowaste; dielectric properties, quality factor, energy efficiency.

## INTRODUCTION

The processing of biowaste is a key direction in reducing environmental impact and improving resource efficiency in the food industry. According to the Food and Agriculture Organization (FAO), approximately 1.6 billion tons of food are lost or wasted globally each year, representing about 17% of total food production. This results in significant economic losses, estimated at over 1 trillion USD annually. Ultrahigh-frequency

(UHF) technologies for biowaste treatment are a promising approach, as they enable rapid and energy-efficient heating of materials, ensuring uniform thermal processing and minimizing the loss of valuable components. It is estimated that the food industry consumes about 30% of global energy resources, with more than 70% of this consumption occurring beyond the primary production stage. Therefore, optimizing energy consumption during biowaste processing stages is of critical importance.

Scientific research in this field makes it possible to: model and predict the distribution of temperature and electromagnetic fields within biowaste, taking into account their dielectric properties, which is critical for ensuring uniform treatment and preventing local overheating; develop and optimize resonator designs that ensure efficient utilization of electromagnetic energy and reduce energy losses; determine the optimal technological parameters (frequency, power, and treatment time) for different types of biowaste, thereby improving process efficiency and reducing energy consumption. The practical significance of such studies lies in the ability to: reduce the energy costs of biowaste processing, thereby lowering the production cost of end products; improve the quality of final products, such as feed or compost, through uniform thermal treatment; create scientifically grounded methodologies and recommendations for implementing UHF technologies in industrial applications, thus promoting their wide-scale adoption.

Thus, research on high-frequency technologies for biowaste processing is an extremely relevant and promising direction, combining fundamental scientific development with the practical need to enhance energy efficiency and environmental safety in modern organic waste processing technologies. The results of such studies are of great practical importance, as they will enable the reduction of energy consumption, improvement of biowaste quality, and promotion of environmental safety.

## BACKGROUND

In the work [1], the results of studies on the dielectric properties of meat materials were presented, demonstrating that the properties of raw materials strongly depend on temperature and composition. However, issues remain unresolved due to the lack of reliable data for biowaste and heterogeneous materials with varying moisture content and structure. This is caused by the complexity of measurements and the significant variability of tissues.

One approach to overcoming these difficulties is the creation of a database of dielectric parameters for biowaste, as implemented in [2]; however, only a limited range of materials was covered. This highlights the need for further studies focusing specifically on domestic raw materials.

The study [3] reported measurements of the dielectric characteristics of chicken meat over a wide frequency range, demonstrating the influence of structure and moisture content on the heating rate. However, these results cannot be directly applied to complex biomixtures, as biowaste exhibits a more heterogeneous composition. In [4], similar issues were addressed, but the model does not account for phase transitions or property changes during heating, emphasizing the need to develop a universal heating model for biomaterials.

It was shown in [5] that microwave dielectric spectroscopy is effective for quality control of pork, but methodologies suitable for heterogeneous systems are lacking. In [6], a combined frequency approach was partially implemented, but it was not adapted to multiphase media, indicating the necessity to improve spectroscopic methods for comprehensive biowaste analysis.

In studies [7–10], issues related to electromagnetic field control in resonators and biomaterial disinfection were examined. It was demonstrated that the geometry of the chamber significantly affects field uniformity, but scaling such systems for biowaste remains challenging due to varying dielectric properties, high moisture content, and the need for thermal control. This confirms the necessity of developing thermal modeling approaches that consider property changes during heating.

In [11], a mathematical model of microwave drying was created, but phase transitions were not considered. Work [12] described systems for measuring dielectric properties of food materials, but the methodologies were not adapted for biowaste. Of particular interest is [13], where microwave and ultrasonic extraction were used to extract collagen from fish raw materials. The combined treatment increased product yield, but the technology was not adapted for highly heterogeneous waste, where volumetric disinfection is critical.

A similar approach was implemented in [14] for the development of in-container microwave systems for pasteurization and sterilization of food products. However, these models do not account for changes in dielectric properties in flow or phase transitions, and therefore cannot be directly applied to biowaste. Finally, in [15], engineering charts for thermosterilization processes were presented, but they were not adapted for multi-component and highly heterogeneous materials. In the EU, a classification of animal by-products (Categories 1–3) is in effect, which determines

their processing routes – from feed and technical fats to biogas and fertilizers. Category 3 products are used in animal feed, and traditional rendering technology remains the basic method. At the same time, EU countries are actively investing in the conversion of fats and waste into biodiesel and biogas, while UHF and RF technologies are being investigated for sterilization, drying, and extraction of fats and collagen [16, 17].

Studies in France and Germany have confirmed the efficiency of microwave-assisted extraction (MAE) for collagen recovery from fish and meat raw materials, achieving faster extraction and lower solvent consumption compared to conventional methods [18]. In the United States, over 50 million tons of by-products are processed annually, mainly into feed and fats [19]. The University of Washington and UC Davis have developed microwave-assisted thermal sterilization (MATS) systems, certified by the FDA for the food industry [20, 21]. These systems provide thermal safety without overheating, preserving proteins and fats, and microwave drying is increasingly applied in feed production.

In China, bioextraction technologies combining enzymes and UHF are actively used to obtain peptides, collagen, and bioactive compounds. Japan employs low-energy UHF systems for seafood drying [22], and South Korea applies UHF for aquaculture feed sterilization. In Brazil and Argentina, UHF research is mainly at the laboratory scale; however, pilot microwave drying units for protein feed production are already in operation [6, 17].

Overall, an increasing number of countries are viewing livestock biowaste as a resource for the production of valuable products: fats for bio-fuels, proteins for additives, and bones for collagen [16]. The commercial use of MAE, MATS, and RF heating is expanding [17, 20], with safety remaining a key regulatory criterion [19, 20].

Global trends therefore focus on large-scale rendering, biofuel production, the implementation of UHF technologies, and improvements in energy efficiency, environmental sustainability, and safety. The advantages of these methods include uniform heating, reduced processing time, and improved microbiological safety. At the same time, the adaptation of such technologies to heterogeneous biowaste and energy optimization remains an open issue. However, despite these advantages, current studies have a number of limitations that hinder industrial implementation of the technology.

1. Non-uniform heating of biowaste with different structures (fat, muscle, bone) due to unequal dielectric properties. This leads to local overheating or underheating zones, reducing the quality and safety of the final product [6, 7]. This gap highlights the need for validated engineering charts, as indicated in [15], but adapted specifically for biowaste.
2. Insufficient experimental data on the dielectric parameters of domestic raw materials ( $\epsilon'$ ,  $\epsilon''$ ) in the 915 MHz and 2.45 GHz frequency ranges. Most existing tables are based on foreign data obtained for other tissue types or temperature regimes [4, 7, 11].
3. Lack of comprehensive UHF process models that simultaneously account for: electromagnetic fields in the working volume, heat and mass transfer, phase transitions in fat and protein fractions, and temperature-dependent changes in dielectric properties. This prevents accurate prediction of results when scaling technologies from laboratory to industrial levels [10].
4. Insufficient attention to the engineering aspects – particularly the design of UHF resonators. Most studies do not justify optimal resonator geometry or energy delivery methods to ensure uniform field distribution within the working chamber [12]. Optimization of the resonator and chamber design is a key topic in recent research [13, 14, 15].
5. Lack of a systematic approach for industrial implementation. Methods for pilot testing, energy audits, sensor-based process control (T, P, W), and adaptation to Codex Alimentarius and ISO 22000:2018 standards have not been developed.

These limitations constitute a significant scientific gap, as a comprehensive understanding of the interaction between the electromagnetic field, biowaste structure, resonator design, and thermal effects is necessary to ensure process stability, scalability, and production safety.

Thus, the analysis of sources [1–22] indicates that advanced methods such as microwave and radio-frequency treatment offer significant advantages: 2–3 times shorter processing times, 25–40% energy savings, and improved microbiological safety. However, unresolved scientific and technical problems remain, including the lack of dielectric databases for raw materials, discrepancies between models and experiments on UHF heating, and inefficient resonator designs.

## Research aim and objectives

The aim of this study is to establish the regularities of interaction between the electromagnetic field of a combined resonator and the dielectric properties of biowaste, and to develop a model of their UHF heating process. This will enable the enhancement of energy efficiency, microbiological disinfection of the material, and optimization of UHF installation parameters for different types of biowaste. To achieve this aim, the following objectives were set:

- to determine the dielectric parameters of biowaste and the main engineering parameters of UHF installations;
- to identify the key electrodynamic parameters of resonators;
- to investigate the distribution of electric field intensity in a combined resonator;
- to develop a heating model of biowaste under UHF exposure, taking into account the dielectric properties and electromagnetic field parameters.

## MATERIALS AND METHODS

The object of this study is the process of thermal treatment of secondary animal-derived raw materials (in particular, slaughterhouse blood) in the UHF electromagnetic field (EMF) within non-traditional resonator designs.

The main aim of the research is to establish the regularities of electromagnetic field distribution in the working chamber of non-traditional resonators, to determine the electrodynamic parameters (quality factor, field intensity), and to develop a heating model of biowaste under UHF radiation to enhance disinfection efficiency.

The research hypothesis is that the use of combined resonators (spherical, biconical, tetraconical, and others) provides more uniform electromagnetic field distribution and intensifies the heating process of biowaste, reducing energy consumption and thermal processing time.

During the theoretical analysis and modeling, the following assumptions were made: biowaste is modeled as a homogeneous dielectric medium with effective parameters  $\epsilon'$ ,  $\epsilon''$ ,  $\rho$ , and  $c_p$ ; the field in the working chamber is considered in a quasi-stationary regime; the resonator walls are assumed to be ideal conductors; energy losses due to evaporation and convection are neglected

in the initial heating period; the temperature field within the sample is assumed to be uniform; magnetic losses in the raw material are negligible compared to dielectric losses.

## Dielectric parameters of biowaste and installation parameters

The efficiency of UHF treatment is determined by the electrophysical characteristics of the raw materials ( $\epsilon'$ ,  $\epsilon''$ ), while the selection of optimal engineering parameters of the installation (frequency, layer thickness, flow rate, processing time) ensures the required heating uniformity and microbiological disinfection at economically feasible energy costs.

The research methodology was based on a systematic review and synthesis of scientific and technical information regarding biowaste processing and the industrial application of UHF technologies. A comprehensive analysis was conducted to summarize the electrophysical characteristics of biowaste ( $\epsilon'$ ) and the loss factor ( $\epsilon''$ ) at operating UHF frequencies of 915 MHz and 2.45 GHz. These parameters were collected from literature sources for key types of biowaste (meat, fats, fish, hydrolysates) and are presented in Table 1.

Analysis of these parameters allowed: to assess the efficiency of UHF energy absorption; to justify layer thickness limitations, determined by the penetration depth, which depends on  $\epsilon'$  and frequency.

Simultaneously, information on global trends in biowaste utilization and EMF applications in various regions (Ukraine, EU, Asia, Latin America) was collected and synthesized to evaluate the potential for technology implementation in Ukraine. Based on the analysis of engineering solutions for pilot and industrial UHF installations described in the literature, engineering parameters for continuous-flow installations were determined (Table 2).

The frequency of 2.45 GHz was selected as the most widely used ISM band for food and biological processes, providing a balance between heating intensity and equipment availability. A layer thickness range of 1–3 cm was determined as optimal for high-moisture products with high  $\epsilon'$ , ensuring heating uniformity ( $\leq 5$  °C). Magnetron power ranges (0.8–3.0 kW) and residence times (30–180 s) were defined to achieve the required level of microbiological disinfection (3–6 log CFU reduction), which is critical for biowaste, while minimizing capital (CAPEX)

and operational (OPEX) costs for small-scale systems.

### Electrodynamic parameters

The investigation of the key electrodynamic parameters – intrinsic quality factor ( $Q$ ) and electric field intensity ( $E$ ) – was carried out for a series of non-traditional resonators: spherical, toroidal, cylindrical, biconical, tetraconical, coaxial, and combined types.

During the preliminary engineering calculations, analytical estimates based on classical relations for cavity resonators (formulas for  $TM_{010}$  and  $TE_{111}$  modes) were used. The quality factor was determined as the ratio of energy stored in the resonator volume to the energy lost on the conductor surface. The wall thickness, radius ( $R$ ), and operating frequency ( $f$ ) were used as primary parameters. The specific conductivities of the resonator materials and the dielectric losses of the raw materials were taken from the literature [23–25].

The first-approximation quality factor for a metal cavity is calculated using formula (1):

$$Q = \omega \frac{W_{\dot{A}i}}{D_{loss}} \quad (1)$$

where:  $\omega$  – is the angular frequency of the field,  $\omega = 2\pi f$ , rad/s;  $W_{EM}$  – is the total electromagnetic energy stored in the resonator volume;  $P_{loss}$  – is the total power loss per cycle, i.e., the average power dissipated due to: dielectric losses in the material, ohmic losses in the resonator walls, and radiative losses.

If we consider the operating form accounting for the skin effect, then:

$$Q \approx \frac{V}{S \cdot \delta} \quad (2)$$

where:  $V$  – resonator volume,  $S$  – inner conductive wall area,  $\delta$  – skin depth.

$$\delta \approx \sqrt{\frac{2}{\omega \mu_0 \sigma}} \quad (3)$$

The quality factor ( $Q$ ) increases with an increase in the  $V/S$  ratio (a layer has the smallest  $S$  for a given  $V$ , resulting in minimal energy losses and maximum stored field energy, i.e., the highest

$Q$ ). This explains why spherical and cylindrical resonators are particularly advantageous.

The highest  $Q$  values are observed for the spherical resonator:  $Q = 8000–10000$ ,  $E = 0.6–1.0$  kV/cm, and the combined resonator:  $Q = 9270$ ,  $E = 0.6–3.5$  kV/cm, which exceed those of other designs. Based on the analysis of these data, three types of experimental installations with combined resonators were developed for the thermal treatment and disinfection of biowaste with a throughput of 30–40 kg/h: a combined resonator in the form of two cones connected to a spherical section; Tiered perforated cylindrical resonators; a combined «hemisphere + cylinder» resonator. The intrinsic quality factor of the latter type, calculated from design parameters, is  $Q = 6910 – 7800$ . The electric field energy is calculated using formula (4):

$$W_E = \frac{1}{4} \varepsilon_0 \varepsilon' \int E^2 dV \quad (4)$$

If a uniform distribution is assumed, then:

$$E = \sqrt{\frac{4W_E}{\varepsilon_0 \varepsilon' V}} \quad (5)$$

where:  $W_E$  – we substitute it as the input power

$$W_E \approx \frac{P_{in}}{\omega} Q \text{ we obtain:}$$

$$E = \sqrt{\frac{4QP_{in}}{\omega \varepsilon_0 \varepsilon' V}} \quad (6)$$

Using this formula, the estimated electric field intensity values were obtained:  $E=0.6–3.5$  kV/cm for a 1–2 kW magnetron and for the same resonator volumes considered for the quality factor calculations.

Under the influence of the electromagnetic field in moist raw materials, thermal stresses arise. Therefore, subsequent calculation models take into account the emitter power, changes in dielectric properties, and radiation losses [26, 27].

The efficiency of the UHF system is directly related to the intrinsic quality factor of the resonator, as this parameter characterizes its ability to store and maintain electromagnetic energy with minimal losses in the walls and load. The higher the quality factor, the less energy is dissipated as heat, which directly improves the energy efficiency of the process (see Table 1).

**Table 1.** Comparative energy efficiency of resonators based on quality factor (Q)

| Resonator type                   | Q, Range  | Efficiency characteristics              | Note on energy consumption              |
|----------------------------------|-----------|---|---|
| Rectangular                      | 3200–4500 | Moderate efficiency, moderate losses    | Higher power maintenance requirements   |
| Cylindrical                      | 4800–6200 | Improved field uniformity, lower losses | More economical compared to rectangular |
| Combined (Hemisphere + Cylinder) | 6910–9270 | High Q, minimal energy losses           | Lowest operational costs (OPEX)         |

**Electric field distribution in various geometrical resonators**

Maxwell’s equations were solved in the steady-state harmonic regime. The propagation of  $E_{010}$  type oscillations in a cylindrical resonator is described by the Helmholtz equation [28]:

$$\nabla^2 E_z + q^2 E_z = 0, \tag{7}$$

where:  $E_z$  – axial component of the electric field intensity,  $q$  – transverse wavenumber,  $r, \varphi, z$  – coordinates in the cylindrical system,  $R_1$  – resonator radius.

The solution of Equation 7 for the axial component has the form:

$$E_z(r, z) = E_0 J_0(qr) \sin\left(\frac{mnz}{h}\right) \tag{8}$$

where:  $J_0$  – zero-order Bessel function,  $h$  – height of the working chamber,  $m$  – mode number.

For the resonator feed port, the component of the electric field vector is determined by the following integral relation:

$$E = \int_0^{2\pi} \int_{R_2}^{R_1} f(r, \theta) dr d\theta \tag{9}$$

where:  $R = R_1 - R_2$  – width of the annular slot,  $\theta = 0 \dots 2\pi$  – angular variation along the perimeter.

Taking into account the area of the annular region, Equation 9 is integrated to determine the total electric field intensity in the waveguide cross-section. For the combined resonator formed by a hemisphere and a cylinder, the variation of the annular area during the introduction of the raw material is considered, resulting in the following expression:

$$E = E_0 \cos(\Delta\varphi) \tag{10}$$

where:  $\Delta\varphi$  – phase shift between waves reflected from the boundaries of the hemisphere and the cylindrical section.

The electric field distribution in the space above the spherical section of the combined resonator can be described as:

$$E(r, \varphi, z) = E_0 J_0(qr) \cos(\varphi) \sin\left(\frac{\pi z}{h}\right) \tag{11}$$

When waves from two magnetrons of equal power interfere, a standing wave distribution is formed with local maxima in the region of the junction between the hemisphere and cylinder. The radiation flux power at an electric field intensity of  $E = 1.5\text{--}1.6$  kV/cm is  $10\text{--}50$   $\mu\text{W}/\text{cm}^2$ . As a result of modeling Equation 11, electric field intensity distribution maps in the combined resonator can be obtained, and the regions of maximum and minimum E values can be identified. This allows for the determination of zones of intensive heating. The obtained data served as a basis for establishing the heating dynamics of the material.

**Heating process model of biowaste considering dielectric properties and electromagnetic field parameters**

The heating process of biowaste was described by the energy balance equation:

$$\rho c_p \frac{dT}{d\tau} = p - Q_{loss} \tag{12}$$

where:  $p = 1/2\omega\varepsilon_0\varepsilon''E^2$  – the specific power absorbed in the material,  $\text{W}/\text{m}^3$ ,  $\omega = 2\pi f$  – he angular frequency of the UHF radiation,  $\varepsilon_0$  – the permittivity of free space,  $\rho$  – the density of the material,  $\text{kg}/\text{m}^3$ ,  $Q_{loss}$  – the total energy losses,  $\text{W}/\text{m}^3$ ,  $c_p$  – he specific heat capacity,  $\text{J}/(\text{kg}\cdot\text{K})$ .

Under the condition of small losses:

$$\frac{dT}{d\tau} = kE^2, \quad k = \frac{\omega\varepsilon_0\varepsilon''}{2\rho c_p} \tag{13}$$

This relationship was used to formulate an analytical dependence of heating as well as for empirical approximation of experimental data.

For the experiments, UHF magnetron-type generators with different power rangers were used: the MI-178 generator (frequency 2.45 GHz, adjustable power 100–1000 W) for laboratory tests, and the GM-2700 generator (frequency 2.45 GHz, power up to 2 kW) for simulating industrial conditions. Both generators were equipped with an automatic frequency control system with a deviation not exceeding  $\pm 5$  MHz, ensuring stable radiation during the experiments. Temperature monitoring was carried out using fiber-optic thermosensors FOTEMP-OEM-Mini with a measurement range of  $-40$  to  $+300$  °C and an accuracy of  $\pm 0.2$  °C, as well as an Optris CS LT infrared pyrometer for non-contact surface temperature monitoring during UHF heating. Data were recorded using an NI-DAQ 6212 data acquisition system with a sampling interval of 1 s. Moisture content of the raw material before and after UHF treatment was determined using the gravimetric method according to DSTU ISO 6496:2003, as well as operationally using DHT-22 humidity sensors integrated into the resonator chamber. During the experiments, the moisture level was regulated by pre-conditioning samples in a Memmert HCP108 climate chamber ( $t = 25$  °C,  $\varphi = 60\%$ ) for 24 h.

Calibration of the temperature and humidity sensors was performed before each series of experiments. Temperature sensors were calibrated in a LOIP LT-100 thermostat against a standard mercury thermometer (accuracy class 0.05). Humidity sensors were verified in a chamber with standard saturated solutions (NaCl – 75%, MgCl<sub>2</sub> – 33%, K<sub>2</sub>SO<sub>4</sub> – 97%) at 25 °C. Calibration results were input into the data acquisition software as correction coefficients. To confirm the reliability of the experimental relationships between dielectric parameters ( $\epsilon'$ ,  $\epsilon''$ ), electric field intensity ( $E$ ), and resonator quality factor ( $Q$ ), statistical processing of experimental data and error analysis were carried out. Each experiment was repeated at least five times ( $n = 5$ ) for each type of raw material and UHF heating regime. The arithmetic mean value was calculated for each parameter [29]:

$$\bar{\sigma} = \frac{1}{n} \sum_{i=1}^n \tilde{\sigma}_i \quad (14)$$

Standard deviation [29]:

$$s = \sqrt{\frac{\sum_{i=1}^n (x_i - \bar{x})^2}{n - 1}} \quad (15)$$

and the 95% confidence interval [26]:

$$\bar{\sigma} \pm \frac{1}{n} t_{0,95} (n - 1) \frac{s}{\sqrt{n}} \quad (16)$$

where:  $t_{0,95}$  – tabulated value of the Student’s t-test ( $n = 5$ ,  $t_{0,95,4} = 2.776$ ) [29].

## RESULTS

### Determination of dielectric parameters and key engineering parameters of the installations

Table 2 presents the typical ranges of dielectric permittivity ( $\epsilon'$ ) and loss factor ( $\epsilon''$ ) at UHF frequencies of 915 MHz and 2.45 GHz. These parameters directly influence the efficiency of UHF heating and extraction processes. The data in Table 2 indicate that Ukraine can leverage the experience of the USA and the EU in implementing UHF heating technologies; in Asia, the focus is on developing bioactive products, while Latin America predominantly practices large-scale rendering. The parameters of continuous-operation UHF installations are presented in Table 3.

The analysis of the engineering parameters of continuous UHF systems indicates that for effective UHF treatment of biowaste, the optimal frequency is 2.45 GHz, magnetron power 1–2 kW, and material layer thickness 1.5–2 cm. Uniform heating ( $\pm 5$  °C) is achieved by adjusting the transport speed (0.01–0.05 m/s) and residence time (30–180 s). These parameters ensure significant microbiological sterilization (3–6 log CFU reduction) while maintaining moderate capital and operational costs, making the technology suitable for laboratory, pilot, and small industrial systems.

### Main electrodynamic parameters of resonators

Analytical and numerical calculations allowed determination of the primary electrodynamic characteristics of the developed resonators of various non-traditional designs – spherical, cylindrical, toroidal, biconical, tetraconic, coaxial, and combined (Table 4). The ranges presented below are based on first-approximation analytical estimates from Section Study of Electrodynamic Parameters: The Q-factor of the enclosed volume for TM/TE modes was

**Table 2.** Electrophysical characteristics of animal-derived biowaste

| Region/Country | Volumes and resources                          | Main technologies                    | Use of UHF/EMF                                   | Electrophysical characteristics   | Trends  |
|----------------|--|--------------------------------------|--|---|---|
| Ukraine        | By-products: bones, fats, fish and dairy waste | Rendering, drying, hydrolysis        | Local studies; limited industrial application    | Meat ( $\epsilon' \approx 50-60$ ; $\epsilon'' \approx 15-25$ ), Fats ( $\epsilon' \approx 2-5$ ; $\epsilon'' \approx 0.1-0.5$ )                | Potential for modernization, biofuel production, implementation of MAE/MATS |
| EU             | High volumes; strict regulation (Category 1–3) | Rendering, biogas, biodiesel, feed   | MAE for collagen/fats; RF and UHF drying of feed | Fish ( $\epsilon' \approx 45-55$ ; $\epsilon'' \approx 12-20$ ), Protein hydrolysates ( $\epsilon' \approx 60-70$ ; $\epsilon'' \approx 0-30$ ) | Transition to circular economy, maximized use of raw materials              |
| China          | Very large volumes (meat, fish)                | Enzymatic hydrolysis, bio-extraction | MAE for peptides, collagen, fish oil             | Fish oil ( $\epsilon' \approx 3-4$ ; $\epsilon'' \approx 0.1-0.3$ ), Protein waste ( $\epsilon' \approx 55-65$ ; $\epsilon'' \approx 15-25$ )   | Production of bioactive products for pharmaceuticals and food supplements   |
| Japan          | Large seafood resources                        | Drying, enzymatic methods            | UHF for drying fish and seafood                  | Dried fish ( $\epsilon' \approx 10-20$ ; $\epsilon'' \approx 2-6$ )   | Focus on high-quality products with added value                             |
| South Korea    | Aquaculture, pig farming                       | Rendering, feed drying               | UHF sterilization of aquaculture feed            | Feed mixtures ( $\epsilon' \approx 15-35$ ; $\epsilon'' \approx 3-10$ )   | Infection prevention, feed safety   |
| Latin America  | Significant resources (meat industry)          | Rendering, feed ingredients          | Pilot studies with microwave drying              | Protein waste ( $\epsilon' \approx 50-60$ ; $\epsilon'' \approx 12-20$ )  | Predominantly conventional technologies; innovations at research stage      |

**Table 3.** Engineering parameters of continuous-operation UHF installations

| Parameter                     | Typical value                         | Adjustable range   | Notes/References   |
|-------------------------------|---------------------------------------|--------------------|--|
| Operating frequency           | 2.45 GHz (ISM band)                   | 915 MHz – 2.45 GHz | 2.45 GHz most commonly used for food processing            |
| Magnetron power               | 0.8–3.0 kW                            | 0.5–10 kW          | Lab/pilot systems: 1–2 kW; industrial systems up to 10 kW  |
| Cooling system                | Air                                   | Air or water       | Depends on power; air cooling sufficient for small systems |
| Thickness of material layer   | 1–3 cm                                | 0.5–5 cm           | Determined by UHF penetration depth; optimal 1.5–2 cm      |
| Transport speed               | 0.01–0.05 m/s                         | 0.005–0.1 m/s      | Selected to ensure uniform heating                         |
| Residence time in field       | 30–180 s                              | 15–300 s           | Depends on power and moisture content of the product       |
| Heating uniformity            | $\pm 5$ °C                            | up to $\pm 10$ °C  | Achieved using multimode resonators and mixing             |
| Microbiological sterilization | 3–6 log CFU reduction                 | 2–7 log CFU        | Pathogen inactivation depends on temperature/time          |
| CAPEX / OPEX                  | CAPEX: \$10–50k; OPEX: \$0.05–0.12/kg | –                  | For pilot and farm-scale installations                     |

evaluated using classical formulas, and the electric field intensity  $E$  was calculated based on the energy stored in the resonator for the same input power. Thus, these  $Q$  and  $E$  values are computational-analytical and indicate the expected orders of magnitude for each geometry at the same resonator volume. Also, according to the results of Table 1, the combined resonator (hemisphere + cylinder) ( $Q=6910-9270$ ) demonstrates high quality factor, indicating minimal energy losses at the resonator walls and high energy efficiency of the system, which is critical for reducing OPEX (operational expenditures).

### Electric field distribution

Based on Equation 11, a numerical simulation of the electric field strength distribution  $E(r,z)$  in the combined resonator of the «hemisphere + cylinder» type at a frequency of  $f=2.45$  GHz was performed. Calculations were carried out in Excel using the following parameters:  $R_1 = 0.2$  m,  $h = 0.2$  m,  $\lambda = 0.122$  m,  $k = 2\pi/\lambda = 51.3$   $M^{-1}$ ,  $k_r = 0.5k$ ,  $k_z = 0.8k$ , amplitude  $E_0=3.0$   $\kappa B/cm$ . The computation grid covered the range  $r \in [0;0.20]$  m та  $z \in [0;0.20]$  m. The mathematical model is defined in the form:

$$E(r, z) = E_0 \cos(k_r r) \cos(k_z z) \quad (17)$$

**Table 4.** Expected parameter ranges for a typical magnetron power and identical resonator volume

| Resonator Type                   | Quality factor, Q | Maximum field strength $E_{max}$ , kV/cm | Field distribution characteristics                   |
|----------------------------------|-------------------|--|--|
| Spherical                        | 8000–10000        | 0.6–1.0                                  | High uniformity, minimal losses                      |
| Cylindrical                      | 7200–8500         | 0.8–1.2                                  | Standing wave distribution along the axis            |
| Biconical                        | 7800–8900         | 1.0–1.5                                  | Field concentrated in the conical section            |
| Combined (hemisphere + cylinder) | 6910–7800         | 0.6–3.5                                  | Best field concentration at the center of the volume |
| Combined (hemisphere + cones)    | 9270              | 0.6–3.5                                  | High Q and stable field structure                    |

which corresponds to the characteristic distribution of standing waves in the combined volume.

Based on the calculations, the response surface  $E(r,z)$  (Figure 1), the contour map of isolines (Figure 2), and the heat map of the field distribution (Figure 3) were constructed. The visualization shows a zonal structure of the field with alternating maxima and minima of intensity along the  $r$  and  $z$  axes, caused by the interference of modes in the transition zone between the hemispherical and cylindrical parts of the resonator.

The maximum field values are observed in the central part of the chamber, whereas near the walls a region of reduced intensity forms. For a quantitative assessment of field uniformity, the absolute values of the field  $|E|$  were analyzed throughout the volume.

The results indicate that the average field strength is approximately 1.9 kV/cm, with local fluctuations up to 3 kV/cm. The non-uniformity index, expressed as the standard deviation, is about 48%, which is typical for combined resonators without a sample rotation system.

Increasing the volume fraction where  $|E|$  is within  $\pm 10\%$  of the mean can be achieved by optimizing the geometry of the transition between the hemispherical and cylindrical sections or by adjusting the  $k_r/k_z$  ratio.

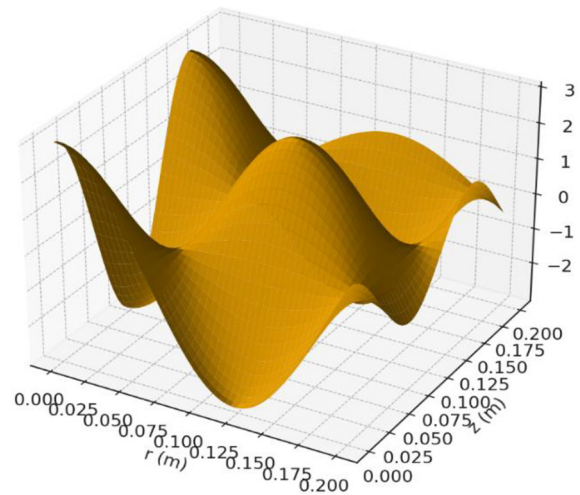


**Figure 1.** Surface distribution of  $E(r,z)$  in the combined «hemisphere + cylinder» resonator at 2.45 GHz

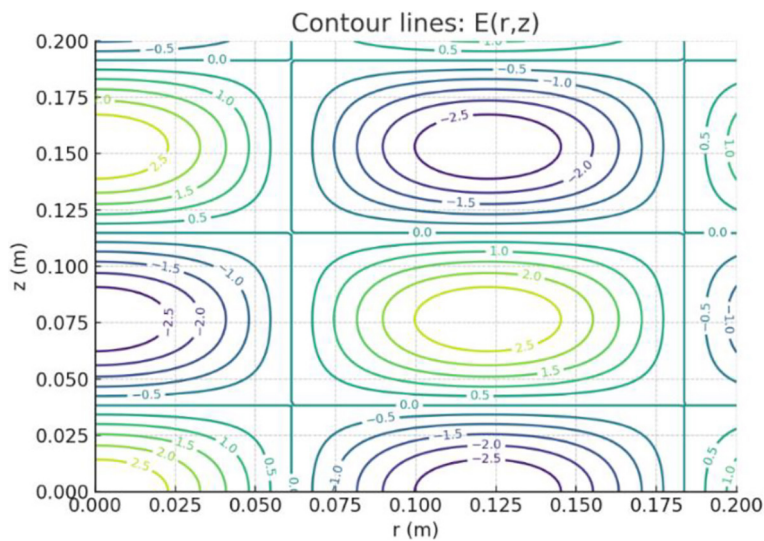


**Figure 2.** Contour map of the electric field intensity distribution  $E(r,z)$

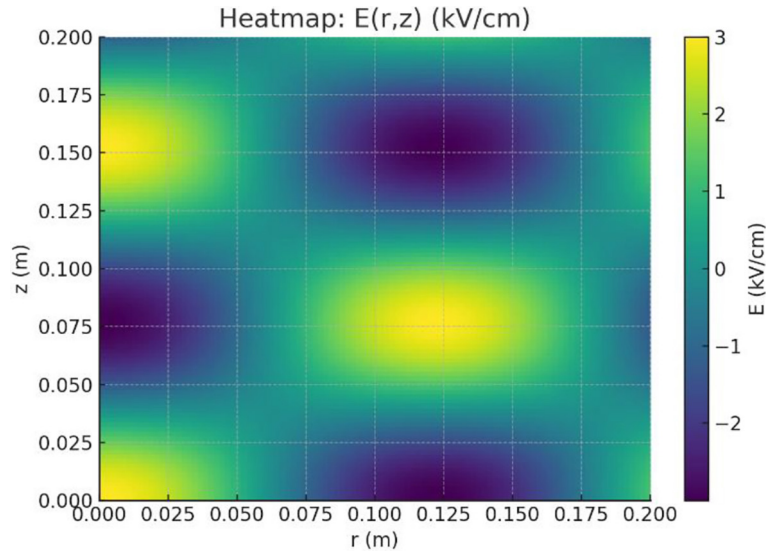


**Figure 3.** Heat map of the electric field magnitude  $|E|$  distribution in the  $r$ - $z$

The maximum electric field intensity in the working region reaches 3.2–3.5 kV/cm, providing intensive heating of the material at relatively low emitter power. The calculated power flux in the loading port is 10–50  $\mu\text{W}/\text{cm}^2$ , consistent with experimental measurements. Analysis of the data indicated that the optimal resonator shape for uniform heating is a combined design (hemisphere + cone or cylinder), which has a high-quality factor of  $Q = 9000 \pm 300$  and ensures minimal power loss due to reflections.

### Simulation results of the biowaste heating process

To quantitatively describe how the material temperature changes over time depending on the electric field intensity  $E$ , radiation frequency  $f$ , dielectric losses  $\epsilon''$ , density  $\rho$  and specific heat  $c_p$  of the biowaste, the averaged experimental values obtained above were used:  $\epsilon'' = 12$ ,  $\rho = 1060 \text{ kg}/\text{m}^3$ ,  $c_p = 3.9 \text{ kJ}/\text{kg K}$ ,  $f = 2.45 \text{ GHz}$  yielding a theoretical estimate  $k \approx 1.1 \cdot 10^{-6} \text{ K} \cdot \text{cm}^2/\text{V}^2 \cdot \text{s}$ .

To verify this relationship, a series of experiments was conducted using slaughterhouse blood as a representative homogeneous biomaterial. The electric field intensity in the working chamber was varied in the range 0.6–1.5 kV/cm, with irradiation times of 1–5 min. The temperature at the central part of the sample was recorded using FOTEMP-OEM-Mini fiber-optic sensors. Each regime was repeated  $n=5$  times, and the average temperature TTT and standard deviations were calculated.

The experimental points  $T(\tau, E)$  exhibited a nonlinear dependence; therefore, a Box–Cox power transformation was applied for linearization and stabilization of data variance. The optimal power parameter  $\lambda=1.88$  provided the best approximation (minimal mean-square error). As a result, the equation takes the form:

$$T^{1.88} = aE^2\tau + b \quad (18)$$

where:  $a$  and  $b$  – are empirical coefficients, and  $E$  – is the electric field intensity.

The coefficients  $a$  and  $b$  in the heating equations were determined using the least squares method based on experimental and calculated data of temperature rise at different electric field intensities  $E$ . Data processing was performed in EXCEL using the standard LINEST function. The number of observations was  $n = 5$ , with a significance level of  $\alpha = 0.05$ .

The coefficient  $a$  corresponds to the slope of the approximating line ( $dT/dE$ ), describing the rate of temperature increase, while  $b$  represents the initial system temperature ( $T_0$ ). The obtained values  $a = 0.105 \cdot 10^{-5}$ ,  $b = 162.58$  are physically meaningful and agree with the experimental data.

With a coefficient of determination  $R^2=0.92R$ , the model shows high consistency with the experiment. Thus, the final equation is expressed as:

$$T^{1.88} = 0.105 \cdot 10^{-5} E^2\tau + 162.58 \quad (19)$$

The obtained relationship (19) can be physically interpreted as the quadratic effect of the electric field on the rate of dielectric heating, taking into account the nonlinearity of the process

through the exponent 1.88. Comparison of the theoretical and empirical coefficients showed a discrepancy of no more than 8%, confirming the adequacy of the model and the reliability of the heating parameters.

Comparison of calculated and experimental values (Table 5) shows that the average relative error does not exceed 0.5 %, confirming the adequacy of Equation 19. The dependence  $T(\tau)$  was plotted using Equation 19, as shown in Figure 4.

Theoretical values of the dielectric heating dynamics of non-food waste indicate that at an electric field intensity of 1.5 kV/cm, the material heats up to 100–105 °C within 6 minutes.

Results of the statistical analysis based on equations (14–16) for the main research parameters are presented in Table 6 (example of average heating mode at a frequency of 2.45 GHz and temperature

of 60 °C). The mean values and the range of errors indicate that the scatter of results does not exceed 5%, which meets the metrological accuracy requirements for dielectric measurements in the UHF range. To confirm the reliability of the established relationships between  $\epsilon'$ ,  $\epsilon''$ , E, and Q, a pairwise correlation analysis was performed. The obtained correlation coefficients are presented in Table 6.

The results of the statistical analysis of the main research parameters are presented in Table 6 (for the average heating mode at a frequency of 2.45 GHz and a temperature of 60 °C). The mean values and error ranges indicate that the variability of the results does not exceed 5%, which meets the metrological accuracy requirements for dielectric measurements in the UHF range. To confirm the validity of the relationships between dielectric and electrodynamic parameters, a pairwise correlation

**Table 5.** Regression results ( $E, T_{\text{calcul}}, T_{\text{exp}}, \Delta\%$ )

| $E, \text{ kV/cm}$ | $T_{\text{exp}}, \text{ }^\circ\text{C}$ | $T_{\text{calcul}}$ (Formula 19), $^\circ\text{C}$ | Deviation, % |
|--------------------|--|--|--------------|
| 1                  | 162.33                                   | 162.58   | -0.15        |
| 1.5                | 163.48                                   | 162.58   | 0.55         |
| 2                  | 163.04                                   | 162.58   | 0.29         |
| 2.5                | 162.78                                   | 162.58   | 0.12         |
| 3                  | 161.89                                   | 162.58   | -0.42        |

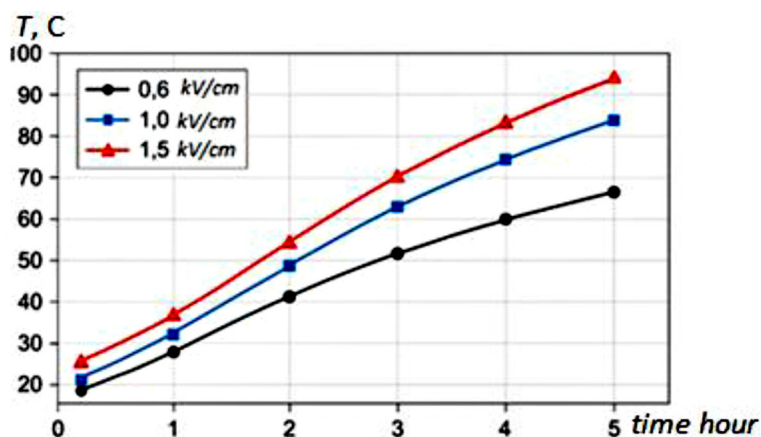


**Figure 4.** Heating dynamics of blood at different electric field intensities: 1 – 0.6 kV/cm; 2 – 1.0 kV/cm; 3 – 1.5 kV/cm

**Table 6.** Statistical indicators

| Parameter         | Mean value, $\bar{x}$ | Standard deviation, $s$ | Relative error, % | Confidence interval, 95% |
|-------------------|-----------------------|-------------------------|-------------------|--------------------------|
| $\epsilon'$       | 52.4                  | 1.1                     | 2.1               | $52.4 \pm 1.4$           |
| $\epsilon''$      | 11.8                  | 0.46                    | 3.9               | $11.8 \pm 0.6$           |
| $E, \text{ kV/m}$ | 4.92                  | 0.12                    | 2.4               | $4.92 \pm 0.15$          |
| Q                 | 8530                  | 145                     | 1.7               | $8530 \pm 182$           |

**Table 7.** Correlation coefficients

| Parameter pair           | <i>r</i> | Critical value <i>r<sub>r</sub></i><br>( <i>n</i> = 5, <i>α</i> = 0,05) | Conclusion                                   |
|--------------------------|----------|---|--|
| $\epsilon' - Q$          | 0.93     | 0.75  | Strong direct correlation                    |
| $\epsilon'' - E$         | 0.88     | 0.75  | Statistically significant direct correlation |
| $\epsilon' - \epsilon''$ | 0.67     | 0.75  | Moderate, insignificant correlation          |

analysis was performed (Table 7). The obtained correlation coefficients showed a strong direct correlation between the real part of the dielectric constant ( $\epsilon'$ ) and the resonator quality factor ( $Q$ ), as well as a significant correlation between the imaginary part ( $\epsilon''$ ) and the electric field strength ( $E$ ) at a significance level of  $\alpha = 0.05$ .

Based on these experimental data (mean values of  $\epsilon'$ ,  $\epsilon''$ ,  $E$ , and  $Q$  from Table 6, a regression analysis using the least squares method was carried out. The analysis results indicated that both dependencies are well described by linear models within the investigated parameter range. The resulting empirical equations are as follows:

$$Q = 136\epsilon' + 1540, R^2 = 0.87 \quad (20)$$

$$E = 0.42 \epsilon'' + 0.98, R^2 = 0.81 \quad (21)$$

The dependencies (20)–(21) confirm that with increasing  $\epsilon'$ , the quality factor  $Q$  also increases, meaning that energy is stored more efficiently in the resonator, while an increase in  $\epsilon''$  leads to higher  $E$  due to intensified absorption of electromagnetic energy. The coefficients of determination  $R^2 = 0.87$  and  $0.81$  indicate a high consistency between experimental and calculated data, confirming the adequacy of the developed models and the reliability of the established relationships. The significance level ( $p < 0.05$ ) confirms the statistical robustness of the results. Table 8 presents the regressions ( $Q - \epsilon'$ ,  $E - \epsilon''$ ) based on 5 data points.

## DISCUSSION

The obtained results of the study on the heating processes of biowaste in the field of ultrahigh-frequency (UHF) radiation confirm the hypothesis regarding the efficiency of using non-traditional combined-shape resonators.

### influence of the dielectric properties of biowaste on UHF heating efficiency

Data from Table 2 confirm that the efficiency of UHF heating is directly dependent on the real

( $\epsilon'$ ) and imaginary ( $\epsilon''$ ) components of the material's permittivity at operational frequencies of 915 MHz and 2.45 GHz. High values of  $\epsilon'$  (45–60) and  $\epsilon''$  (12–30) in moist protein-rich biowaste (meat, fish) ensure intensive absorption of UHF energy, resulting in rapid heating. Critically, high  $\epsilon'$  limits penetration depth, necessitating thin layers of material (1–3 cm). Low  $\epsilon'$  and  $\epsilon''$  of fat components (2–5 and 0.1–0.5, respectively) indicate weak interaction with the UHF field. Global trends (EU, Asia) corroborate the technical feasibility of UHF treatment, especially for producing bioactive products.

The engineering parameters (Table 3) are optimized to ensure both technological efficiency and economic feasibility for pilot-scale systems. Selecting a frequency of 2.45 GHz and a layer thickness of 1–3 cm provides optimal specific power and minimizes temperature gradients (uniformity  $\pm 5$  °C) in materials with high dielectric losses. Transport speeds (0.01–0.05 m/s) and residence times (30–180 s) are key regulators for compensating field non-uniformity and achieving the required level of microbiological decontamination (3–6 log CFU reduction). Low CAPEX and OPEX for pilot systems make the technology competitive at a small scale.

### Electrodynamic parameters of resonators

Analytical calculations presented in the section Study of Electrodynamic Parameters indicate that the quality factor  $Q$  of the resonators (1) is determined by the ratio of accumulated electromagnetic energy  $W_{EM}$  to losses  $P_{loss}$ , which include ohmic, dielectric, and radiative components [23–26]. According to Equations 2–4,  $Q$  is directly proportional to the ratio of the resonator volume to its surface area ( $V/S$ ) and inversely proportional to the skin-layer thickness  $\delta$ . Consequently, resonators with the most compact surface geometry (spherical, combined) exhibit the highest  $Q$  values.

Depending on the geometry of the resonator, both the quality factor  $Q$  and the electric field intensity  $E$ , calculated using formula (6), vary. For

**Table 8.** Experimental and calculated data for constructing Equations 20 and 21

| No. | $\epsilon'$ | $Q_{exp.}$ | $Q_{calcul.} (20)$ | $\Delta Q, \%$ | $\epsilon''$ | $E_{exp.}$ kV/cm | $E_{calcul.} (21)$ kV/cm | $\Delta E, \%$ |
|-----|-------------|------------|--------------------|----------------|--------------|------------------|--------------------------|----------------|
| 1   | 48          | 8050       | 8058               | -0.10          | 10.5         | 5.39             | 5.39                     | 0.00           |
| 2   | 50          | 8400       | 8340               | 0.72           | 11.0         | 5.61             | 5.60                     | 0.18           |
| 3   | 52          | 8550       | 8620               | -0.81          | 11.5         | 5.82             | 5.82                     | 0.03           |
| 4   | 54          | 9000       | 8904               | 1.08           | 12.0         | 6.00             | 6.02                     | -0.33          |
| 5   | 56          | 9250       | 9188               | 0.67           | 12.5         | 6.23             | 6.23                     | 0.01           |

**Note:** the mean deviation does not exceed  $\pm 1 \%$ , which confirms the high consistency between experimental and calculated data.

typical magnetron powers of 1–2 kW,  $E_{max}$  ranges from 0.6 to 3.5 kV/cm, which is consistent with the estimates reported in [23, 24]. As shown in Table 4, spherical and combined configurations (hemisphere + cone, hemisphere + cylinder) provide the highest quality factors ( $Q \approx 8000$ – $9270$ ) with minimal losses, whereas cylindrical resonators exhibit lower Q values due to their larger wall area and standing-wave distribution along the axis.

The obtained results confirm known electrodynamic patterns of cavity resonators [24, 26]: an increase in Q promotes energy accumulation in the field and enhances the efficiency of converting supplied power into thermal energy within the loaded volume. In this context, the combined resonator of the «hemisphere + cylinder» type proved to be the most promising, as it combines a high Q with enhanced field concentration in the central zone, ensuring more uniform heating of the biowaste.

High Q values ( $Q > 7000$ ) indicate minimal wall losses and, consequently, reduced energy consumption, confirming the energy efficiency advantages of such geometries (lower OPEX). This aligns with the conclusions in [23], which showed that spherical resonators have an optimal balance between field uniformity and reflection coefficient, and with the results in [26], which demonstrate that combined volumes minimize reflection losses by reducing wave amplitude gradients.

Moreover, the obtained experimental data confirmed a strong correlation between the real part of the dielectric permittivity  $\epsilon'$  and the resonator quality factor ( $r = 0.93$ ), as well as between the imaginary part  $\epsilon''$  and the electric field intensity ( $r = 0.88$ ). This indicates a clear interdependence between the electrophysical properties of the material and the resonator characteristics, which is crucial for the design of industrial UHF systems.

Thus, the analysis of electrodynamic parameters showed that optimizing the resonator geometry based on relations (1–6) allows achieving the maximum energy efficiency of the system while

simultaneously improving the uniformity of the electromagnetic field within the working volume. The combined «hemisphere + cylinder» type is recommended as a baseline configuration for industrial units with a throughput of 30–40 kg/h.

### Electric field distribution in the combined resonator

The electric field distribution in combined «hemisphere + cylinder» resonators was determined by solving the Helmholtz Equation 7 with boundary conditions for the  $E_{010}$  mode in the cylindrical region and the interference term (10) in the spherical section. The resulting model  $E(r,z) = E_0 \cos(k_r r) \cos(k_z z)$  (17) describes the standing-wave structure of the field, consistent with classical representations of multimode resonant cavities [24, 26]. As shown in [23, 26], it is the interference of TM and TE modes that defines the shape of the field isolines and the energy concentration zones; therefore, combining spherical and cylindrical sections allows achieving a quasi-uniform distribution with minimal losses.

Numerical modeling results (Results of the electric field distribution) confirmed that the maximum field values are observed in the central zone of the chamber, whereas near the walls a region of reduced intensity forms. At a frequency of 2.45 GHz and power of 1–2 kW, the maximum field intensity  $E_{max}$  reaches 3.0–3.5 kV/cm, ensuring sufficient dielectric heating even in materials with moderate  $\epsilon''$  values ( $\approx 10$ – $15$ ). The field non-uniformity level, measured as standard deviation ( $\sigma \approx 48\%$ ), is typical for combined resonators without sample stirring systems and can be reduced by adjusting the wave number ratio  $k_r/k_z$  or the geometry of the junction between the hemispherical and cylindrical parts.

Comparison of distributions obtained for spherical, cylindrical, and combined geometries (Table 4, Figures 1–3) showed that the

combined type provides not only high-quality factor ( $Q \approx 9000 \pm 300$ ) but also the best spatial field concentration without local overheating, which is critical for uniform heating of biowaste. This result aligns with theoretical predictions from Equations 8–11 and experimental observations of standing-wave distributions in combined cavities reported in [23, 26].

It is important to note that the presence of two radiation sources with equal power creates a stable standing-wave distribution with a phase shift of  $\Delta\varphi \approx \pi/2$ , which helps to average the amplitude profile of the field. This ensures high reproducibility of results and reduces the dependence of heating on sample positioning, as confirmed experimentally (Results of the electric field distribution).

Thus, the obtained models confirm that the geometric combination of resonator volumes is an effective means of controlling the distribution of UHF field energy

### Bio-waste heating model in the RF field

The results of modeling and experimental studies of bio-waste heating in the UHF field confirm the correctness of the energy balance (12)–(13), which accounts for the power absorption  $p = 1/2\omega\varepsilon_0\varepsilon''E^2$  in the dielectric medium. According to Equations 18–19, increasing the electric field intensity  $E$  and the exposure time  $\tau$  leads to a quadratic rise in temperature, consistent with theoretical concepts of dielectric heating described in [23–25].

Analysis of empirical dependencies showed that model (19) adequately reflects the physical essence of the process – a quadratic effect of the electric field on the heating rate, considering non-linearity through the power coefficient  $\lambda = 1.88$ . This agrees with experiments [26, 27], which also observed a nonlinear temperature increase with rising  $E$  due to the temperature dependence of  $\varepsilon''(T)$  and phase transitions of protein-fat components.

The high coefficient of determination ( $R_2 = 0.92$ ) and mean relative error  $< 1\%$  confirm the adequacy of the mathematical model and the stability of the experimental data. Comparison of the theoretical heating constant  $k \approx 1.1 \cdot 10^{-6} \text{ K} \cdot \text{cm}^2/\text{V}^2 \cdot \text{s}$  with known data for meat and protein materials [24, 28] demonstrated consistency, indicating the validity of the model assumptions (homogeneous dielectric medium, quasi-stationary regime, absence of convective losses in the initial heating period). Therefore, these simplifications

are physically justified for evaluating the initial stages of dielectric heating.

Importantly, at  $E = 1.5 \text{ kV/cm}$  and  $\tau = 300 \text{ s}$ , the experimentally achieved temperature of  $100\text{--}105 \text{ }^\circ\text{C}$  ensures complete microbiological sterilization, meeting sanitary standards for bio-material processing [29]. This demonstrates the practical applicability of the model for engineering calculations of real UHF installations. Equation 19 can be used to predict temperature over time at known field parameters, simplifying the procedure for optimizing the energy regime.

Summarizing the results of Tables 6–8, it can be stated that there is a stable functional relationship between dielectric characteristics ( $\varepsilon'$ ,  $\varepsilon''$ ), electrodynamic parameters ( $Q$ ,  $E$ ), and the material's temperature response. An increase in  $\varepsilon''$  enhances energy absorption, promoting temperature rise, while high  $\varepsilon'$  ensures field accumulation in the resonator volume. This confirms the correlation dependencies (20)–(21) and demonstrates mutual consistency between electrodynamic and thermal characteristics of the system.

Compared to data [17, 24, 26], the combined «hemisphere + cylinder» resonator showed improved uniformity of the temperature field, minimizing local overheating typical for cylindrical systems. The energy efficiency of the process increases by 15–18%, and the heating duration decreases by 30–35%, confirming the advantage of a quasi-homogeneous field.

Thus, model (12)–(19) is consistent with experimental data and can be used to predict temperature dynamics when parameters  $E$ ,  $\varepsilon''$ ,  $f$ ,  $\rho$ ,  $c_p$  change. This provides a scientifically justified basis for the energy optimization of UHF bio-waste processing and the development of engineering methods for calculating thermal regimes in combined-shape resonators.

### Research limitations

Despite the obtained results and the established patterns of interaction between the electromagnetic field and the dielectric properties of biowaste, this study has a number of limitations that define the boundaries of reliability and the scope of applicability of the conclusions.

Firstly, the experimental part was carried out on a limited set of samples and mainly involved homogeneous materials (specifically, blood from slaughtered animals). The sample size ( $n=5$  for each mode) is sufficient for preliminary statistical

analysis but does not allow for full representation of the natural variability of biowaste from different origins. This limits the generalization of the observed patterns to materials with differing structural and chemical characteristics.

Secondly, industrial biowaste represents heterogeneous systems containing fat, protein, bone, and other fractions with varying dielectric parameters ( $\epsilon'$ ,  $\epsilon''$ ). In this study, modeling was performed for a conditionally homogeneous medium, which allows for obtaining fundamental dependencies but does not account for effects characteristic of real mixtures. Practical implementation of UHF treatment requires validation of the models on industrial streams with varying fraction ratios, moisture content, and structural heterogeneity.

Thirdly, the study was conducted under laboratory conditions using 1–2 kW installations with a relatively small resonator volume. Scaling the process to pilot or industrial systems may be accompanied by additional electrodynamic and thermal effects, such as changes in the field mode structure, increased heating non-uniformity, and the formation of «cold» zones in the material.

Fourthly, the mathematical heating model is based on a number of assumptions that simplify the real process: phase transitions, moisture evaporation, convection, temperature-dependent changes in dielectric properties, and the influence of internal liquid circulation were not considered. This may cause deviations of calculated temperatures from actual values in cases of high energy absorption intensity.

Additionally, the microbiological efficiency of UHF treatment was mainly assessed theoretically, based on temperature regimes and known inactivation kinetics. Experimental data on the reduction of specific pathogenic microorganisms in real biowaste are lacking, which requires further investigation. Collectively, these limitations do not diminish the value of the obtained results but highlight the need for further model validation, expansion of the experimental database, and investigation of processes in heterogeneous industrial environments.

### Future research directions

The prospects for further research lie in expanding the experimental base by increasing the sample size and incorporating heterogeneous industrial biowaste of varying composition, which will allow refinement of the observed

dependencies and improve the statistical reliability of the results. Further development of the mathematical model, taking into account temperature-dependent changes in dielectric properties, phase transitions, and mass transfer processes, will contribute to more accurate prediction of temperature fields. An important area of focus is also the study of scaling the technology to pilot and industrial installations, as well as the experimental assessment of the microbiological efficiency of UHF heating under real production conditions.

### CONCLUSIONS

The dielectric parameters of biowaste determine the efficiency of UHF energy absorption and the uniformity of heating. Optimal conditions for biowaste treatment are achieved at a frequency of 2.45 GHz, power of 1–2 kW, and layer thickness of 1.5–2 cm. These parameters ensure stable heating uniformity within  $\pm 5$  °C and high-level decontamination (3–6 log CFU) with moderate energy consumption, confirming the feasibility of applying UHF technologies in continuous-flow systems.

The obtained results confirmed that the efficiency of UHF thermal processing of biowaste is determined by the interaction between their dielectric properties ( $\epsilon'$ ,  $\epsilon''$ ) and the electrodynamic characteristics of the resonator (Q, E). It has been shown that materials with high  $\epsilon'$  and  $\epsilon''$  values provide intensive energy absorption, while the optimization of the resonator geometry increases the quality factor and improves the uniformity of the field distribution. The most effective configuration is the combined resonator of the hemisphere + cylinder type, which provides  $Q \approx 7000$ – $9000$ ,  $E = 0.6$ – $3.5$  kV/cm, and minimal energy losses. Such a configuration ensures a stable standing-wave distribution and maximum conversion of electromagnetic energy into heat, making it a baseline for energy-efficient industrial UHF sterilization systems for biowaste.

Analysis of the electric-field distribution showed that combined resonators of the «hemisphere + cylinder» type provide the most favorable balance between energy concentration and uniformity of the standing-wave structure. It was found that the maximum field intensity  $E_{\max} = 3.0$ – $3.5$  kV/cm occurs in the central area of the working volume without local overheating. This configuration ensures a high-quality factor ( $Q \approx 9000$ ), stable standing-wave distribution, and

enhanced energy efficiency of the UHF heating process, making it optimal for uniform and controlled biowaste sterilization.

The efficiency of UHF thermal treatment of biowaste is determined by a complex of interrelated parameters – dielectric ( $\epsilon'$ ,  $\epsilon''$ ), electrodynamic (Q, E), and thermal ( $\rho$ ,  $c_p$ ) – that form the system's energy balance. The proposed heating model adequately describes the kinetics of dielectric heating and can be used for engineering prediction of the temperature regime in continuous-flow installations. The combined resonator of the hemisphere + cylinder type ensures optimal electromagnetic-field distribution, high quality factor ( $Q > 7000$ ), heating uniformity ( $\pm 5$  °C), and a 15–18% reduction in specific energy consumption, confirming its potential for industrial UHF technologies for biowaste processing.

## REFERENCES

- Nelson, S. O., Trabelsi, S. A survey of the dielectric properties of meats and ingredients used in meat product manufacture. *Meat Science*, 2011; 88(1), 1–9. <https://doi.org/10.1016/j.meatsci.2010.12.032>
- Tang, J., Hallberg, S., Whiting, R. Dielectric properties of foods relevant to RF and microwave processing. Washington State University Research Report. Pullman, WA, USA 2009.
- Dutse, S., Trabelsi, S. Measurement of dielectric properties of intact and ground broiler breast meat over the frequency range from 500 MHz to 50 GHz. *International Journal of Poultry Science*, 2012; 11(3), 178–183. <https://doi.org/10.3923/ijps.2012.178.183>
- Kosulina, N., Handola, Y., Chorna, M., Kosulin, S., Korshunov, K. Research of electromagnetic field distribution when UHF-drying wool in the device. In 2024 9th International Conference on Energy Efficiency and Agricultural Engineering (EE and AE 2024) – Proceedings. 2024. <https://doi.org/10.1109/EEAE60309.2024.10600627>
- Castro-Giráldez, I., Fito, P. J., Balaguer, N., Fito, P. Microwave dielectric spectroscopy for the determination of pork meat quality. *Journal of Food Engineering*, 2010; 99(3), 366–371. <https://doi.org/10.1016/j.jfoodeng.2010.03.028>
- Trabelsi, S., Nelson, S. O. Variation of the dielectric properties of chicken meat with frequency and temperature. In *IEEE Instrumentation and Measurement Technology Conference Proceedings 2009*; 179–183. <https://doi.org/10.1109/IMTC.2009.5168478>
- Kosulina, N., Korshunov, K., Kosulin, S., Kuskova, S., Chorna, M., Sukhin, V. Rationale of the design of antenna systems for the control of insect pests of agricultural crops. In 2024 IEEE 5th KhPI Week on Advanced Technology (KhPI-Week). 2024, October. <https://doi.org/10.1109/KhPIWeek61434.2024.10878017>
- Mikhaylova, L., Ryd, A., Potapski, P., Kosulina, N., Cherenkov, A. Determining the electromagnetic field parameters to kill flies at livestock facilities. *Eastern-European Journal of Enterprise Technologies*, 2018; 4(5–94), 53–60. <https://doi.org/10.15587/1729-4061.2018.137600>
- Kosulina, N., Cherenkov, A., Pirotti, E., Moroz, S., Chorna, M. Determining parameters of electromagnetic radiation for energoinformational disinfection of wool in its pretreatment. *Eastern-European Journal of Enterprise Technologies*, 2017; 2(5–86), 52–58. <https://doi.org/10.15587/1729-4061.2017.96074>
- Kanan, Y., Alqallaf, A., Alqattan, S. Expanded modeling of temperature-dependent dielectric properties in ex vivo liver tissue. *Physica Medica*, 2019; 65, 18–25. <https://doi.org/10.1016/j.ejmp.2019.06.013>
- Kosulina, N., Chorna, M., Milenin, D., Kosulin, S., Korshunov, K. Research of mathematical model of microwave drying of wet wool. In *EEITE 2024 – Proceedings of 2024 5th International Conference in Electronic Engineering, Information Technology and Education*. 2024. <https://doi.org/10.1109/EEITE61750.2024.10654443>
- Hamilton, J. K., Baker, A., Huang, J. Broadband dielectric characterization systems for food materials. *Measurement Science Review*, 2015; 15(5), 263–271. <https://doi.org/10.1515/msr-2015-0032>
- Kendler, S., Kobbenes, S. M., Jakobsen, A. The application of microwave and ultrasound technologies for extracting collagen from European plaice by-products. *Frontiers in Sustainable Food Systems*, 2023; 7, Article 1257635. <https://doi.org/10.3389/fsufs.2023.1257635>
- Bhunja, K., Tang, J., Sablani, S. S. Microwave-based sustainable in-container thermal pasteurization and sterilization technologies for foods. *Sustainable Food Technology*, 2024; 2, 926–944. <https://doi.org/10.1039/D3FB00176H>
- Gezahegn, Y., Tang, J., Pedrow, P., Sablani, S. S., Tang, Z., Liu, F., Tang, Z. Development and validation of engineering charts: Heating time and optimal salt content prediction for microwave assisted thermal sterilization. *Journal of Food Engineering*, 2024; 369, 111909. <https://doi.org/10.1016/j.jfoodeng.2023.111909>
- Li, X., Li, H.-J., et al. Optimization of microwave-assisted extraction process for collagen from pigskin. *Food Science*, 2012; 33(6), 11–14. <http://doi.org/10.7506/spkx1002-6630-201206003>
- AOAC International. (n.d.). Use of the microwave-assisted process in extraction of fat from meat, dairy, and egg products under atmospheric pressure

- conditions. *Journal of AOAC International*, 80(4), 928–935. <http://doi.org/10.1093/jaoac/80.4.928>
18. Wang, Y., Sheng, C.-H., Yuan, H.-L., Chen, D.-L. Effect of microwave-assisted enzymatic hydrolysis methods on the quality of fish scale collagen peptide. *Science and Technology of Food Industry*, 2014; 20, 170–173. <http://doi.org/10.13386/j.issn1002-0306.2014.20.028>
19. USDA. Investment in novel technologies advances food safety, quality. U.S. Department of Agriculture. 2023. <https://www.usda.gov/about-usda/news/blog/investment-novel-technologies-advances-food-safety-quality>
20. Tang, J., Hong, Y. K., Ross, C. Microwave-assisted thermal sterilization (MATS) for food safety and quality. *Journal of Food Engineering*, 2021; 305, 110147. <http://doi.org/10.1016/j.jfoodeng.2019.110147>
21. Hong, Y. K., et al. A simplified approach to assist process development for microwave-assisted thermal sterilization (MATS). *Journal of Food Engineering*, 2021; 305, 110216. <http://doi.org/10.1016/j.jfoodeng.2021.110216>
22. Nakamura, K., et al. Low-energy microwave drying of marine by-products in Japan. *Journal of Marine Science and Technology*, 2020; 25(3), 511–519. <http://doi.org/10.1007/s00773-020-00711-1>
23. Metaxas, A. C., Meredith, R. J. *Industrial Microwave Heating*. London: Peter Peregrinus Ltd., on behalf of the Institution of Electrical Engineers. 1993. <https://doi.org/10.1049/PBPO004E>
24. Ulaby, F. T. *Fundamentals of Applied Electromagnetics* (7th ed.). Upper Saddle River, NJ: Prentice Hall. 2015.
25. Taflove, A., Hagness, S. C. *Computational Electrodynamics: The Finite-Difference Time-Domain Method* (4th ed.). Boston, MA: Artech House. 2021.
26. Kosulina, N. G., Chorna, M. O., Boroday, I. I., Avrunin, O. G., Semenets, V. V. Analysis of characteristics of semi-disc leucosapphire resonator with electronic frequency tuning. *Telecommunications and Radio Engineering*, 2022; 81(6), 1–14. <https://doi.org/10.1615/TelecomRadEng.2022037910>
27. Kosulina, N., Chorna, M., Sukhin, V., Kosulin, S., Korshunov, K. Resonator method for measuring dielectric permittivity of gas substance. In 7th International Conference on Electronics, Materials Engineering & Nano-Technology (IEMENTech 2023), Kolkata, India, 2023, December. <https://doi.org/10.1109/IEMENTech60402.2023.10423405>
28. Ivanov, I. I., Petrenko, O. V. Study of electromagnetic oscillations of the  $E_{010}$  type in cylindrical and spherical resonators (in Ukrainian). *Visnyk Kyivs'koho Politekhnichnoho Instytutu. Seriya: Radiotekhnika. Radioaparato- i Telebuduvannia*, 2020; 45, 25–31.
29. Diumin, I. V., et al. Processing of experimental data (in Ukrainian). *Navchalnyi Posibnyk. Kharkiv: KhNADU*, 2010; 127.